Clim. Past Discuss., 7, 943–964, 2011
www.clim-past-discuss.net/7/943/2011/
doi:10.5194/cpd-7-943-2011

Climate of the Past Discussions

Distinct responses of East Asian summer and winter monsoons to orbital forcing

Z. Shi[1], X. Liu[1], Y. Sun[1], Z. An[1], Z. Liu[2], and J. Kutzbach[2]

[1]Institute of Earth Environment, Chinese Academy of Sciences, Xi'an, China
[2]Center for Climatic Research, University of Wisconsin-Madison, Madison, Wisconsin, USA

Received: 30 December 2010 – Accepted: 19 February 2011 – Published: 7 March 2011

Correspondence to: Z. Shi (shizg@ieecas.cn)

Published by Copernicus Publications on behalf of the European Geosciences Union.

Abstract

Influences of the Earth's orbital forcing on the evolution of East Asian monsoon have been demonstrated with various geological records and climate models. Here, we present time series of climatic proxies from the Chinese Loess Plateau and Sanbao/Hulu caves and the winter/summer monsoon intensity index from a long-term transient climate model simulation. Both the observations and modeling results reveal consistently distinct responses of East Asian summer and winter monsoons to orbital forcing. Different from the dominant local impact on the summer monsoon at the precession scale (~ 20 ka period), the East Asian winter monsoon is driven predominantly by the obliquity forcing (~ 40 ka period). We propose that the obliquity forcing controls the meridional insolation difference and therefore exerts a more significant effect on the evolution of the East Asian winter monsoon than expected before.

1 Introduction

The development of East Asian monsoon (EAM) is closely linked to global climate change and exerts a profound influence upon living environments in the most populous regions in the world. The seasonal reversal in the regional atmospheric circulation is traditionally considered to be driven by the ocean-land thermal contrasts, which is resulted from the seasonal variations of solar radiation. According to modern monsoon theory (Wang, 2006), the robust Siberian high, a heat-driven high-pressure cell, occupies widely inland regions in the Eurasian continent, and draws cold-dry northwesterly outflows from the Asian continental interior during winter seasons, inducing an arid environment in the Northern China. While in summer, the monsoon is anchored by the Asian Low and brings abundant vapor mainly from the Northwest Pacific and plentiful rainfall in East Asia (Fig. 1).

The EAM reconstructions on the geological timescale will help much to understand how the EAM evolves in the past and provide useful information for the prediction for

CPD
7, 943–964, 2011

the future, thus, has already attracted many researchers' attention (e.g., Ding et al., 1992; An et al., 2001; Wang et al., 2005). The evolution of EAM, including the summer and winter monsoons, has long been accepted to be well documented in the eolian deposits on the Chinese Loess Plateau (An et al., 1991; An, 2000). Recently, the stalagmite oxygen isotope records with absolute-dating from caves have provided high-resolution variability of the summer monsoon (Yuan et al., 2004; Wang et al., 2008). The EAM system is fundamentally influenced on the orbital scale by both direct insolation forcing and variations in global ice volume. In the last 800 000 years, a strong 100-ka period consistent with global ice volume cycles is clearly found in the grain size records of Chinese loess, which indicates that the EAM system might be dominated by the changes in glacial-age boundary conditions (Ding et al., 1995).

Since debates still exist as to the mechanisms how the glacial cycles occur (Hays et al., 1976), researchers generally focus on the precession and obliquity periodic bands when evaluating the effect from orbital insolation. Some studies argue that global climate is linearly responded to orbital-driven variation in radiation budget on these two bands (Imbrie et al., 1992) and the EAM development is associated to the local insolation in the Northern Hemisphere(NH) (Yuan et al., 2004; Wang et al., 2008). Owing to its dominant role in the insolation variation, precession has been widely emphasized as the key factor (Clemens and Prell, 2003; Wang et al., 2008). However, how the orbital parameters affect the EAM on these two bands still needs to be clarified.

General circulation model (GCM) simulations are also widely applied to explain the evolution of Asian monsoon (e.g., Kutzbach et al., 1981; Braconnot et al., 2002; Liu et al., 2003). A large number of modeling studies simulate combined precession and obliquity signals in the monsoon systems, where precession dominates obliquity effects. Due to the huge computational costs of GCM operations, however, previous paleomonsoon experiments are equilibrium and focused on certain time-slices. For example, the Paleoclimate Modelling Intercomparison Project (PMIP) has only provided "snapshots" on climate in two special periods of 6 ka BP and 21 ka BP. With the prescribed boundary conditions, e.g., the ice sheet and orbital parameters, the climatic

CPD
7, 943–964, 2011

responses have obtained after the models reach equilibrium. This restriction would lead to the absence for analyzing long-term transient response of climate system and comparing directly with time series of geological climatic proxies. As the development of acceleration technique, it is possible for us to simulate the long-term continuous response of climate system to time-dependent orbital forcing (Jackson and Broccoli, 2003; Lorenz and Lohmann, 2004). Especially, a 284-ka transient simulation with a fully-coupled ocean-atmosphere GCM is employed recently in order to explore the effects of insolation (Kutzbach et al., 2007).

In this paper, the distinct responses of East Asian summer and winter monsoons to orbital forcing and possible driving mechanisms are proposed. Two series of EAM proxies are employed to show the difference between summer and winter monsoons and the long-term evolutionary simulation results are analyzed for further discussions. In Sect. 2, the EAM proxies and modeling results are first introduced. The responses of summer and winter monsoons and their mechanisms are analyzed and discussed in Sects. 3 and 4, respectively. The main points are finally concluded in Sect. 5.

2 Geological records and modeling data

A set of high-resolution EAM variability records covering approximately the last two/three glaciation cycles are employed for this study. For the summer monsoon, the absolute-dated speleothem oxygen isotope records from Sanbao and Hulu caves (Fig. 1) in Central China are chosen for the period of the past 224 000 years (Wang et al., 2008). Fluctuations in the stalagmite δ^{18}O largely reflect changes in δ^{18}O values of atmospheric precipitation, and in turn, relates to changes in the summer monsoon strength (Yuan et al., 2004). Three grain size (GS) records of Chinese loess, which is widely used as a proxy for changes in the intensity of the East Asian winter monsoon (Xiao et al., 1992), are respectively from Jingyuan (Sun et al., 2006a), Xifeng-Changwu (Guo et al., 2009) and Zhaojiachuan (Sun et al., 2006b) sections (Fig. 1). The grain-size model (Porter and An, 1995) is used instead of orbital tuning method to calculate

CPD
7, 943–964, 2011

the age of successive stratigraphic layers to reduce the prescribed information about orbital periods. For our purpose, the 100-ka eccentricity component (greater than 67-ka) has already been filtered out.

Modeling outputs from a fast ocean-atmosphere model (FOAM) are employed to explore evolutionary responses of monsoon systems to orbitally-included changes of insolation (Kutzbach et al., 2007). FOAM is a fully coupled global climate model without using flux adjustment. In previous studies, FOAM has well simulated most major features of global monsoon systems (Liu et al., 2004). In order to accelerate long-term simulations, a well-validated orbital forcing accelerating scheme is used (Jackson and Broccoli, 2003; Lorenz and Lohmann, 2004). With a factor of 100, FOAM was actually run for a length of 2840 simulated years after spin-up. That is, the orbital parameters are advanced by 100 years at the end of each simulated year (Kutzbach et al., 2007). Other boundary conditions, including the global ice sheets, are kept at the same as present day. Hence, the simulated variations of EAM during the past 284 ka, which covers approximately 12 precession cycles or 7 obliquity cycles, can be used to analyze the time-dependent response to orbital forcing. The "calendar effect", which means changes in length of months and seasons that occur with the changing season of perihelion, is not taken into account in the current study.

Due to the delay of climate systems, the climate responses often lag the insolation forcing for a few months. For example, with the minimal insolation in December, the sea level pressure maximum over land often occurs in January in our simulation. Hence, the simulated Siberian winter high (Asian summer low) during December-January-February (June-July-August) are employed as indicators of winter (summer) monsoon intensity and the in-phase December (June) insolation is chosen for comparisons. Spatial domains of pressure cells are defined as follows: Siberian High: 30–70° N, 60–130° E, Asian Low: 25–40° N, 70–110° E. The composite differences are defined on the precession and obliquity bands respectively as the averages between (1) the average of ten model years with minimal precession (PL, maximal insolation in boreal summer) minus those with maximal precession (PH, minimal insolation in boreal

CPD
7, 943–964, 2011

summer) in each precession cycle; (2) the average of ten model years with maximal obliquity (TH, maximal insolation) minus those with minimal obliquity (TL, minimal insolation) in each obliquity cycle.

3 EAM responses to orbital forcing

3.1 Time-dependent responses

The responses of the East Asian summer and winter monsoons are shown in the time series of climatic proxies from geological records (Fig. 2). During the past 224 ka, the stalagmite δ^{18}O values, considered as the proxy of the summer monsoonal precipitation, change synchronously with precession, revealing an obvious 20-ka periodicity (Fig. 2a). The in-phase relation supports the hypothesis that the subtropical summer monsoon systems respond directly to precession-dominated changes in NH insolation (Kutzbach et al., 1981). On the precession scale, stronger summer monsoon is found to appear with the maximal insolation. Different from the δ^{18}O values, however, three GS variations does not follow the precession well and only a weak precession signal is visibly detected. In contrast, the GS records vary more synchronously with the obliquity (Fig. 2b), with a period of about 40-ka, which indicates that the development of the winter monsoon might differ from that of the summer monsoon.

Similar responses with the geological records are also detected in the summer/winter monsoon indices during the period of our simulation (Fig. 3). In summer, a dominant 20-ka precession cycle is observed in the variation of Asian low pressure (Fig. 3a), which is consistent with the local insolation. The approximately out-of-phase relation indicates that the intensified Asian low pressure system corresponds to stronger local insolation at the precession band which tends to induce a strengthened ocean-land thermal difference. In addition, a slight phase difference between the pressure and δ^{18}O values (Figs. 2a, 3a) appeals that variation of EAM, as indicated by the monsoon proxies, lags changes in the pressure cells. Despite the fact that the 20-ka cycle is still

CPD
7, 943–964, 2011

a little visible, the winter monsoon index is dominated by the 40-ka obliquity forcing with a phase leading the GS variations (Fig. 3b).

Variance percentages of different orbital components for both geological proxies and simulated monsoon index are presented in Table 1. The variability of Asian summer monsoon is dominated by the precession forcing, reaching fractions of 52% and 82% respectively for geological proxies and simulated indices, which is consistent with the referenced 30° N June insolation (92%). In boreal winter, precession can still control the variability of 50° N insolation (46%) although the contribution from obliquity significantly increases (35%). But a larger variance of obliquity component consistently indicate more contribution from obliquity than precession in the Asian winter monsoon variability, which differs from local insolation. Thus, the response of East Asian winter monsoon is quite different from that of the summer monsoon, which is primarily influenced by the obliquity forcing.

3.2 Composite differences

The distinct responses of EAM to orbital forcings are illustrated by the composite differences for the surface air temperature (Fig. 4), sea level pressure (SLP, Fig. 5), surface wind (Fig. 6) and precipitation rate (Fig. 7) during boreal summer (JJA) and winter (DJF) at precession and obliquity bands.

With an increase in the precession-induced summer insolation (corresponding to decreased precession), the composite difference of surface air temperature shows that a cold anomaly of 0.5 °C is exhibited over subtropical Pacific in boreal summer (Fig. 4a). However, the surface air temperature increases by about 1 °C over the East Asian continent, with a maximum of up to 4 °C over Far East region, which significantly intensify the ocean-land thermal contrast over East Asia. In boreal winter, the monsoon response becomes distinctly converse. The air temperature is reduced by 2 °C on the colder land but the cooling might be restricted to the mid-latitude regions (Fig. 4c). On the obliquity band, a similar pattern is shown in both responses during summer and

CPD
7, 943–964, 2011

winter that the air temperature remarkably decreases in the high latitudes as obliquity increases while the change is less significant in the tropics (Fig. 4b, d).

Following the surface air temperature changes, the SLP also varies as a result of intensified land-ocean thermal contrast by precession (Fig. 5a, c). The composite differences of SLP show that two prominent pressure anomalies occur over East Asian monsoon region. In boreal summer, a low SLP anomaly is located at the continent where the surface temperature is remarkably enhanced. The other high pressure anomaly develops over the ocean with anomalous surface wind divergence (Fig. 5a). On the obliquity scale, the patterns of SLP changes also correspond well to that of surface temperature. As the obliquity increases, the SLP over the high latitudes has significantly enhanced (Fig. 5b, d) due to the surface cooling (Fig. 4b, d).

In response to the strengthened SLP difference, the southeasterly surface wind has been obviously intensified by about $4\,m\,s^{-1}$ over Eastern China when the summer insolation reaches its peak on the precession band (Fig. 6a), which indicates a linear response of the summer monsoon system to precession forcing. However, the summer monsoon does not change significantly with the increasing obliquity (Fig. 6b). In boreal winter, the intensified high pressure cells over high latitudes induce stronger winter monsoons, represented by intensified northwesterly wind over Northeastern China, however, the monsoon response is more significant on the obliquity band than precession (Fig. 6c, d). The summer precipitation increases by about $2\,mm\,d^{-1}$ and $0.3\,mm\,d^{-1}$ over Eastern China respectively for the precession and obliquity bands as a result of intensified monsoon system (Fig. 7a, b). In boreal winter, rather than on the precession scale (Fig. 7c), the obliquity-scale monsoon enhances and moves southward and brings plentiful frontal rainfall to Southeastern China (Fig. 7d), appealing the importance of obliquity forcing in the evolution of winter monsoon.

CPD
7, 943–964, 2011

4 Proposed mechanisms

As shown above, the East Asian summer and winter monsoons exert distinct responses to orbital forcings. The summer monsoon is no doubt predominantly driven by the precession, which supports the idea that the tropical/subtropical summer monsoon is controlled by the local insolation (Figs. 3a, 8). The larger insolation enhances the regional land-ocean thermal contrast and thus induces a stronger summer monsoon. However, the response of winter monsoon is quite different, exhibiting a more obvious 40-ka period than 20-ka period, suggesting more influences from obliquity. In the following, we try to propose possible mechanisms for such obliquity-controlled winter monsoon.

It is clear that precession enhances the seasonal contrast in one hemisphere and controls the major changes in solar radiation over each latitudes of the earth. Different from the dominance of precession in the tropical insolation, the contribution from obliquity increases in the high-latitude areas (Fig. 8). For example, precession can explain about 92% of the variability of the 30° N June insolation (Table 1). But for the 50° N June insolation, the fraction of precession decreases to 46% and that of obliquity increases to 35%. Compared with the low pressure centre in summer, the location of high pressure cell of winter monsoon system moves northward. The zonal ocean-land thermal contrast led by 50° N insolation has certainly affected on the development of the Siberian High and induces a larger contribution from obliquity on the winter monsoon system (Fig. 8). However, other factors are still required to explain why stronger obliquity signals are detected than precession in the winter monsoon response.

We propose the distinct effect of obliquity parameter on insolation that leads to the remarkable 40-ka signals. Although precession controls the variability of insolation, obliquity forcing determines the meridional insolation differences between the hemispheres. Physically, with the southward shift of ITCZ in boreal winter, more solar radiation at the low latitudes of the southern ocean leads to an upward airflow and that produces the Australian Low. The thermal-induced cross-equatorial meridional

CPD
7, 943–964, 2011

circulation, with a strong downward current over Eurasian continent, may substantially affect the development of the Siberian High. Thus, the ratio of insolations at 20° S and 50° N (approximately the center at Australian Low and Siberian High, respectively) is considered here as an indicator for the intensity of meridional circulation. This index is found to vary in a period of 40 ka, consistent with the response of the Siberian High (Figs. 3b, 8). Therefore, besides the local insolation forcing, the large-scale cross-equatorial circulation, which is resulted from the inter-hemisphere meridional insolation contrast, also play an important role on the Asian winter monsoon. Similar with our results, a previous study also indicated that obliquity-driven differential heating between low and high latitudes, which controls the poleward flux of heat and moisture, may exert the dominant control on high-latitude climates (Raymo and Nisancioglu, 2003).

5 Conclusions

Newly developed climatic proxies from caves in Central China and the Chinese Loess Plateau and an indicator of the EAM intensity from a 284 ka long-term transient GCM simulation have both revealed distinct responses of East Asian summer and winter monsoons to orbital forcing, at least in the past two or three glacial cycles. In boreal winter, other than the generally-accepted importance of local insolation, the atmospheric circulation driven by meridional thermal contrast also has a substantial influence on the Siberian High and then leads to an obliquity-periodic monsoon evolution. The Asian summer monsoon, however, is mainly controlled by the precession-induced local insolation and the corresponding ocean-land temperature contrast. Hence, these distinct responses imply that obliquity-driven meridional thermal contrast, as far not mentioned before, may have significant influence especially on the evolution of the East Asian winter monsoon.

CPD
7, 943–964, 2011

Acknowledgements. The study is jointly supported by NSFC (41075067), the 973 Program (2011CB403406), Innovation Program of Chinese Academy of Sciences (KZCX2-EW-114) and NSFC (40825008).

References

An, Z. S.: The history and variability of the East Asian paleomonsoon climate, Quaternary Sci. Rev., 19, 171–187, 2000. 945

An, Z. S., Kukla, G., Porter, S. C., and Xiao, J. L.: Magnetic susceptibility evidence of monsoon variation on the Loess Plateau of Central China during the last 130 000 years, Quaternary Res., 36, 29–36, 1991. 945

An, Z. S., Kutzbach, J. E., Prell, W. L., and Porter, S. C.: Evolution of Asian monsoons and phased uplift of the Himalaya-Tibetan Plateau since late Miocene times, Nature, 411, 62–66, 2001. 945

Braconnot, P., Loutre, M. F., Dong, B., Joussaume, S., and Valdes, P.: How the simulated change in monsoon at 6 ka BP is related to the simulation of the modern climate: results from the Paleoclimate Modeling Intercomparison Project, Clim. Dynam., 19, 107–121, 2002. 945

Clemens, S. C. and Prell, W. L.: A 350 000 year summer monsoon multi-proxy stack from the Owen Ridge, Northern Arabian Sea, Mar. Geol., 201, 35–51, 2003. 945

Ding, Z. L., Rutter, N. W., Han, J. T., and Liu, T. S.: A coupled environmental system formed at about 2.5 Ma over East Asia, Palaeogeogr. Palaeocl., 94, 223–242, 1992. 945

Ding, Z. L., Liu, T. S., Rutter, N. W., Yu, Z. W., Guo Z. T., and Zhu, R. X.: Ice-volume forcing of East Asian winter monsoon variations in the past 800 000 years, Quaternary Res., 44, 149–159, 1995. 945

Guo, Z. T., Berger, A., Yin, Q. Z., and Qin L.: Strong asymmetry of hemispheric climates during MIS-13 inferred from correlating China loess and Antarctica ice records, Clim. Past, 5, 21–31, 2009, http://www.clim-past.net/5/21/2009/. 946

Hays, J. D., Imbrie, J., and Shackleton, N. J.: Variations in the Earth's orbit: pacemaker of the Ice Ages, Science, 194, 1121–1132, 1976. 945

Imbrie, J., Boyle, E. A., Clemens, S. C., Duffy, A., Howard, W. R., Kukla, G., Kutzbach, J., Mar-

CPD

7, 943–964, 2011

tinson, D. G., McIntyre, A., Mix, A. C., Molfino, B., Morley, J. J., Peterson, L. C., Pisias, N. G., Prell, W. L., Raymo, M. E., Shackleton, N. J., and Toggweiler, J. R.: On the structure and origin of major glaciation cycles. 1. Linear responses to Milankovitch forcing, Paleoceanography, 7, 701–738, 1992. 945

Jackson, C. S. and Broccoli, A. J.: Orbital forcing of Arctic climate: mechanisms of climate response and implications for continental glaciation, Clim. Dynam., 21, 539–557, 2003. 946, 947

Kutzbach, J. E.: Monsoon climate of the early Holocene: climate experiment with Earth's orbital parameter for 9000 years ago, Science, 214, 59–61, 1981. 945, 948

Kutzbach, J. E., Liu, X. D., Liu, Z. Y., and Chen, G. S.: Simulation of the evolutionary response of global summer monsoons to orbital forcing over the past 280 000 years, Clim. Dynam., 30, 567–579, doi:10.1007/s00382-007-0308-z, 2007. 946, 947

Liu, Z., Otto-Bliesner, B., Kutzbach, J., Li, L., and Shields, C.: Coupled climate simulation of the evolution of global monsoons in the Holocene, J. Climate, 16, 2472–2490, 2003. 945

Liu, Z., Harrison, S. P., Kutzbach, J. E., and Otto-Bliesner, B.: Global monsoons in the mid-Holocene and oceanic feedback, Clim. Dynam., 22, 157–182, 2004. 947

Lorenz, S. J. and Lohmann, G.: Accelerated technique for Milankovitch type forcing in a coupled atmosphere-ocean circulation model: method and application for the Holocene, Clim. Dynam., 23, 727–743, 2004. 946, 947

Porter, S. C. and An, Z. S.: Correlation between climate events in the North Atlantic and China during the last glaciation, Nature, 375, 305–308, 1995. 946

Raymo, M. E. and Nisancioglu, K.: The 41 kyr world: Milankovitch's other unsolved mystery, Paleoceanography, 18(1), 1011, doi:10.1029/2002PA000791, 2003. 952

Sun, Y. B., Chen, J., Clemens, S. C., Liu, Q. S., Ji, J. F., and Tada, R.: East Asian monsoon variability recorded by a loess sequence from the Northwestern Chinese Loess Plateau, Geochem. Geophy. Geosy., 7, Q12Q02, doi:10.1029/2006GC001287, 2006a. 946

Sun, Y. B., Clemens, S. C., An, Z. S., and Yu, Z. W.: Astronomical timescale and palaeoclimatic implication of stacked 3.6-Myr monsoon records from the Chinese Loess Plateau, Quaternary Sci. Res., 25, 33–48, 2006b. 946

Wang, B.: The Asian Monsoon, Springer Publishing Company, New York, 2006. 944

Wang, P. X., Clemens, S., Beaufort, L., Braconnot, P., Ganssen, G., Jian, Z., Kershaw, P., and Sarnthein, M.: Evolution and variability of the Asian monsoon system: state of the art and outstanding issues, Quaternary Sci. Rev., 24, 595–629, 2005. 945

CPD
7, 943–964, 2011

Wang, Y. J., Cheng, H., Edwards, R. L., Kong, X., Shao, X., Chen, S., Wu, J., Jiang, X., Wang, X., and An, Z.: Millennial- and orbital-scale changes in the East Asian monsoon over the past 224 000 years, Nature, 451, 1090–1093, 2008. 945, 946

Xiao, J. L., Zheng, H. B., and Zhao, H.: Variation of winter monsoon intensity on the Loess Plateau, Central China during the last 130 000 years: evidences from grain size distribution, Quaternary Res., 31, 13–19, 1992. 946

Yuan, D. X., Cheng, H., Edwards, R. L., Dykoski, C. A., Kelly, M. J., Zhang, M., Qing, J., Lin, Y., Wang, Y., Wu, J., Dorale, J. A., An, Z., and Cai, Y.: Timing, duration, and transitions of the last interglacial Asian Monsoon, Science, 304, 575–578, 2004. 945, 946

CPD
7, 943–964, 2011

Table 1. Variance percentages of orbital components for both geological climatic proxies and model simulated indices of East Asian summer and winter monsoons (precession component: 18–25 ka bandpass-filtered; obliquity component: 33–50 ka bandpass-filtered). The grain size data from Jingyuan(J)/Xifeng-Changwu(X)/Zhaojianchuan(Z) sections are respectively shown for winter monsoon. The referenced 30° N June (50° N December) insolation for summer (winter) monsoon is also included. See more details in the text.

EAM summer (winter: J/X/Z)	Precession	Obliquity
Geological proxies	52% (31%[a]/25%[a]/14%[a])	11% (52%[a]/51%[a]/57%[a])
Simulated indices	82% (17%)	0.0[b] (32%)
Local insolation	92% (46%)	3% (35%)

[a] 100-ka eccentricity component (greater than 67-ka) has been filtered out.
[b] Not significant at 0.9 confidence level.

CPD
7, 943–964, 2011

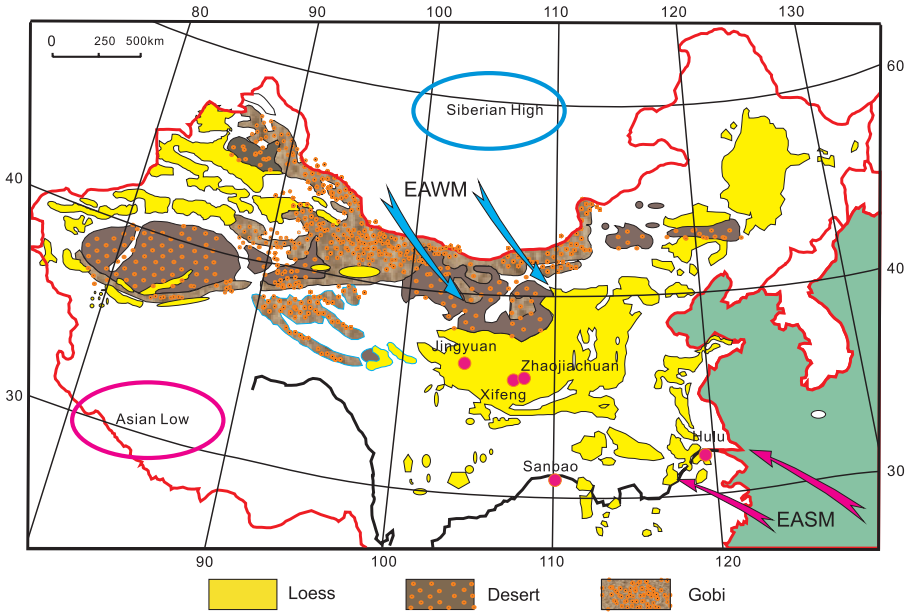

Fig. 1. Map showing the atmospheric circulation regime in East Asia and the locations of the sites in our study. EASM – East Asian summer monsoon, EAWM – East Asian winter monsoon.

CPD
7, 943–964, 2011

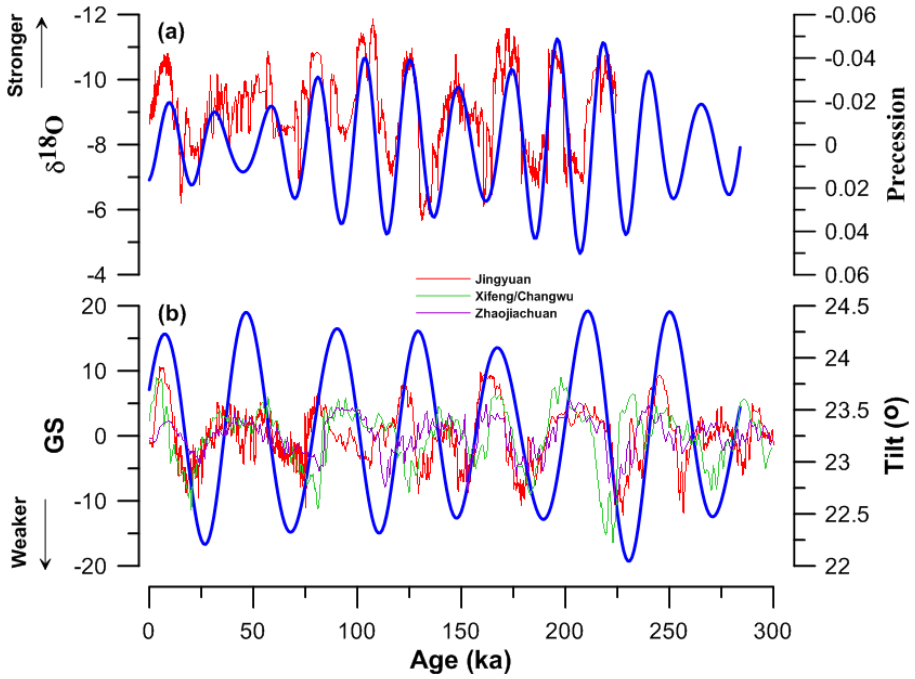

Fig. 2. Proxy records of East Asian monsoon evolution. **(a)** The absolute-dated stalagmite δ^{18}O record from Sanbao and Hulu caves in Central China during the past 224 ka (red). The parameter of precession is plotted for comparison (blue). **(b)** Three grain size records of Chinese loess from Jingyuan(red)/Xifeng-Changwu(green)/Zhaojianchuan(purple) sections covering the past 300 ka, plotted on arbitrary scale. The 100-ka component (greater than 67 ka) has been filtered out. The parameter of obliquity is plotted for comparison (blue).

CPD
7, 943–964, 2011

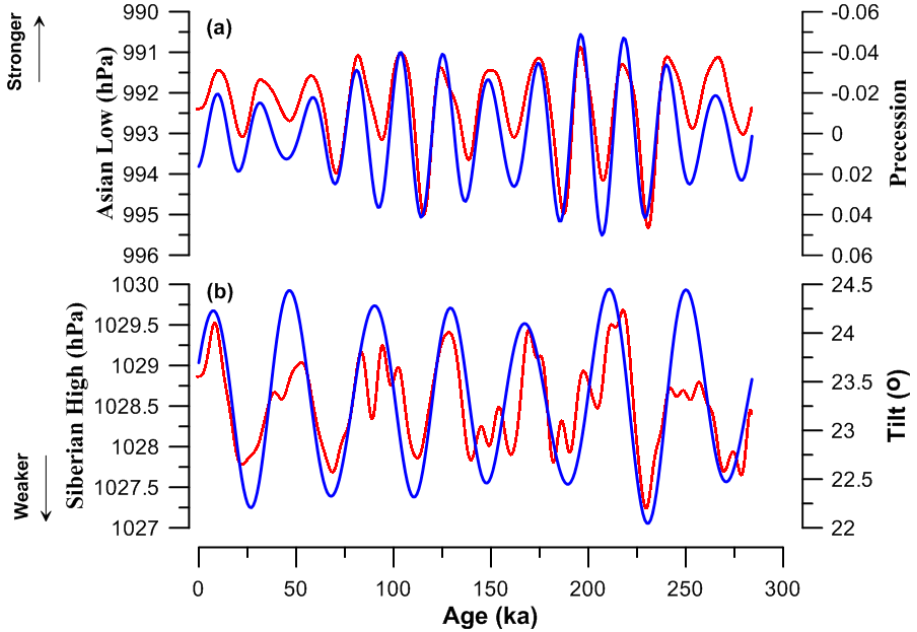

Fig. 3. Simulated time-dependent responses of East Asian summer and winter monsoons during the past 284 ka. The monsoon indices are defined as the averaged sea-level pressure for the Asian Low region (25–40° N, 70–110° E) in boreal summer (JJA) and for the Siberian High region (30–70° N, 60–130° E) in boreal winter (DJF), respectively. The components with periods of less than 10 ka have been filtered out.

CPD
7, 943–964, 2011

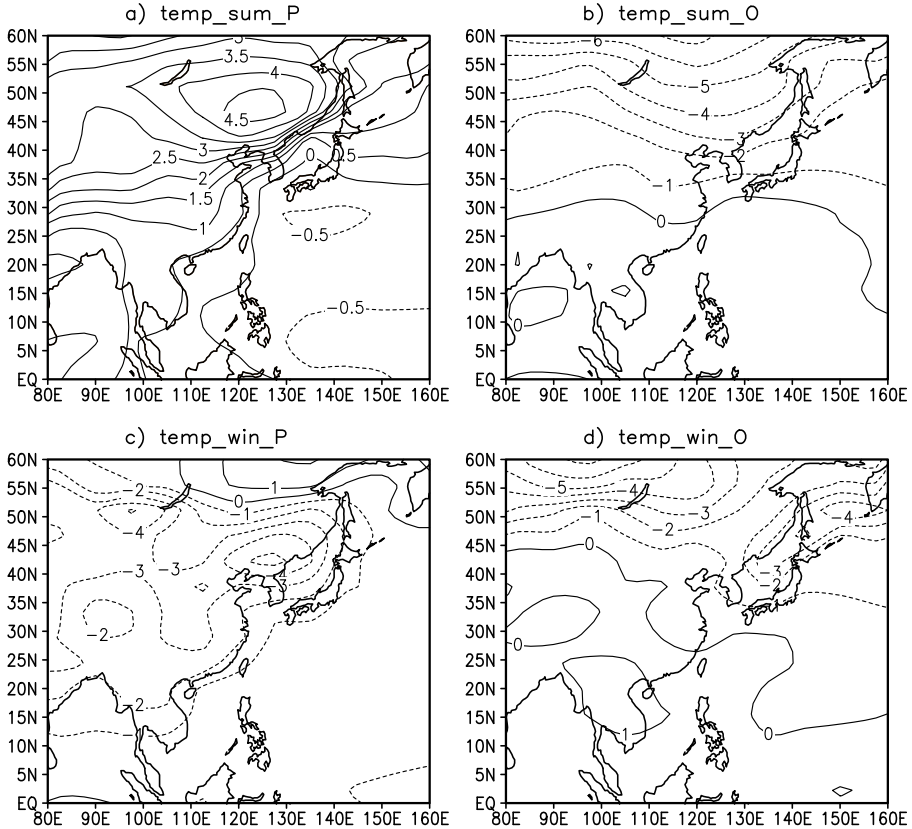

Fig. 4. Composite differences for surface air temperature (°C) over East Asia on the precession (left, PL-PH) and obliquity (right, TH-TL) bands: **(a, b)** summer (JJA); **(c, d)** winter (DJF). See more in the text.

CPD
7, 943–964, 2011

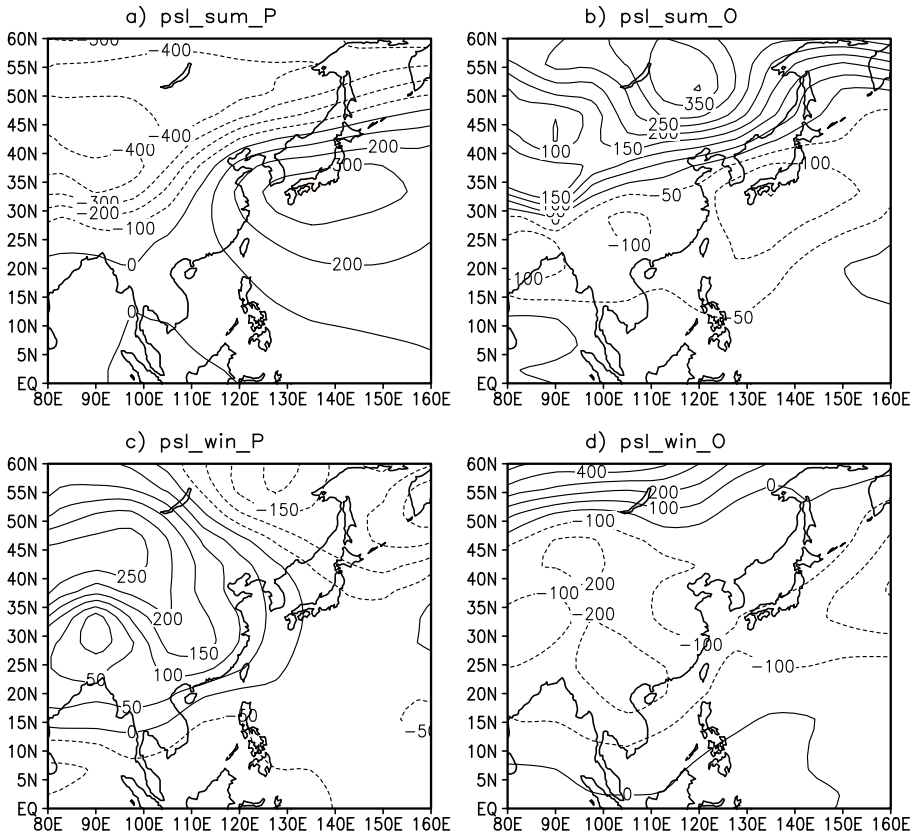

Fig. 5. Same as Fig. 3, but for sea level pressure (hPa).

CPD
7, 943–964, 2011

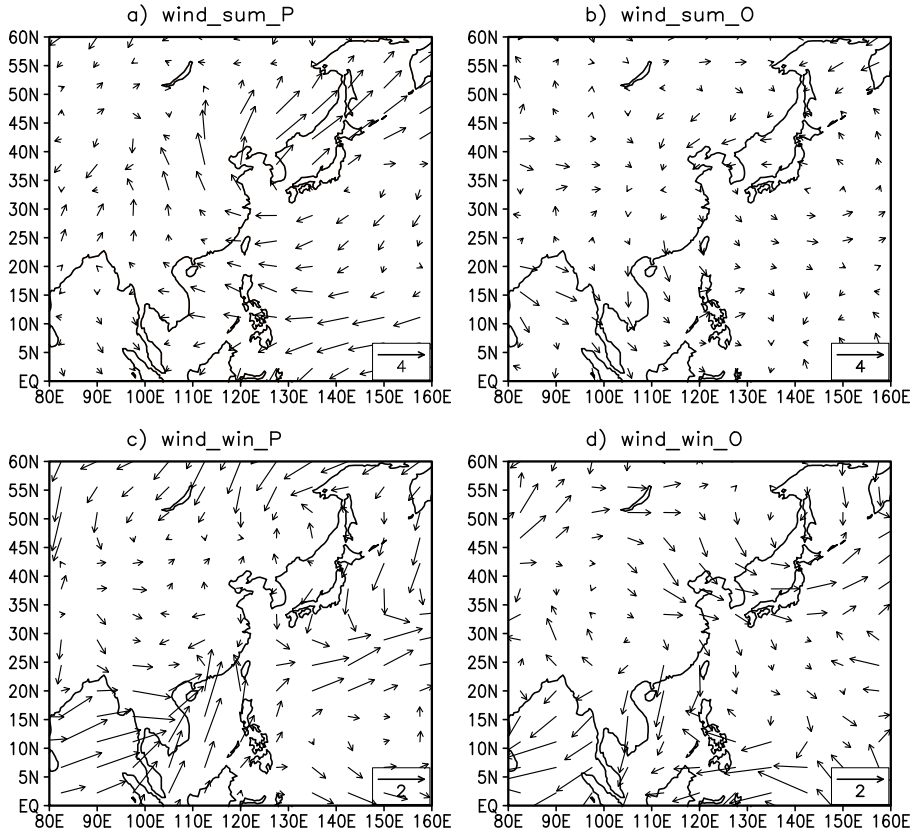

Fig. 6. Same as Fig. 3, but for surface wind vectors ($m\,s^{-1}$).

CPD
7, 943–964, 2011

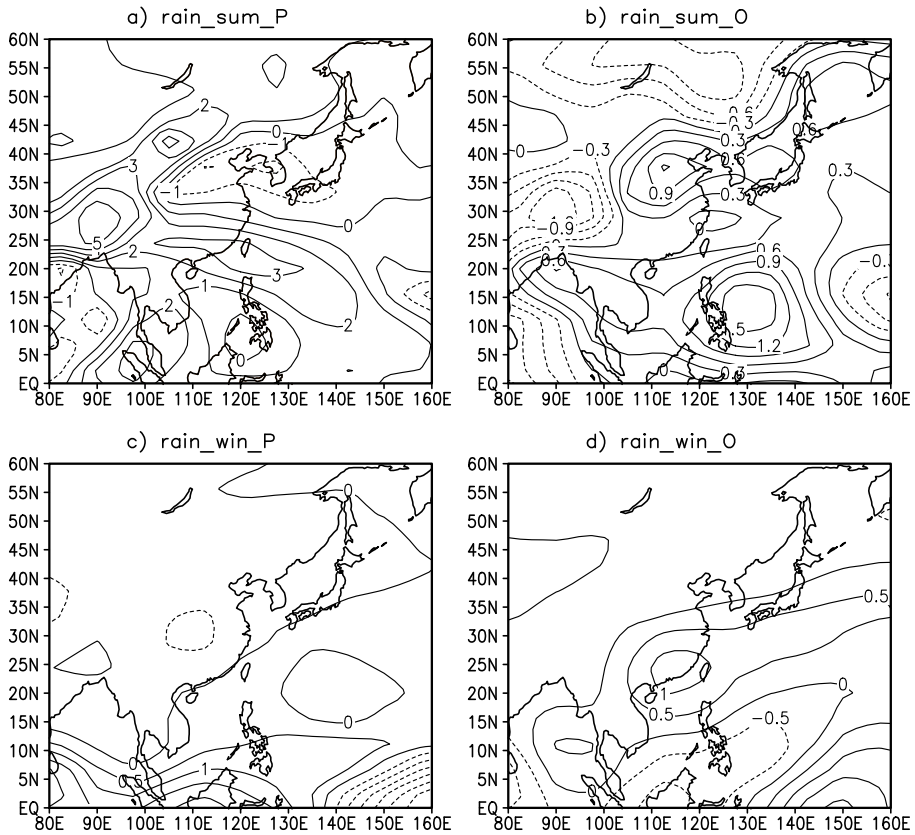

Fig. 7. Same as Fig. 3, but for precipitation rate (mm d^{-1}).

CPD
7, 943–964, 2011

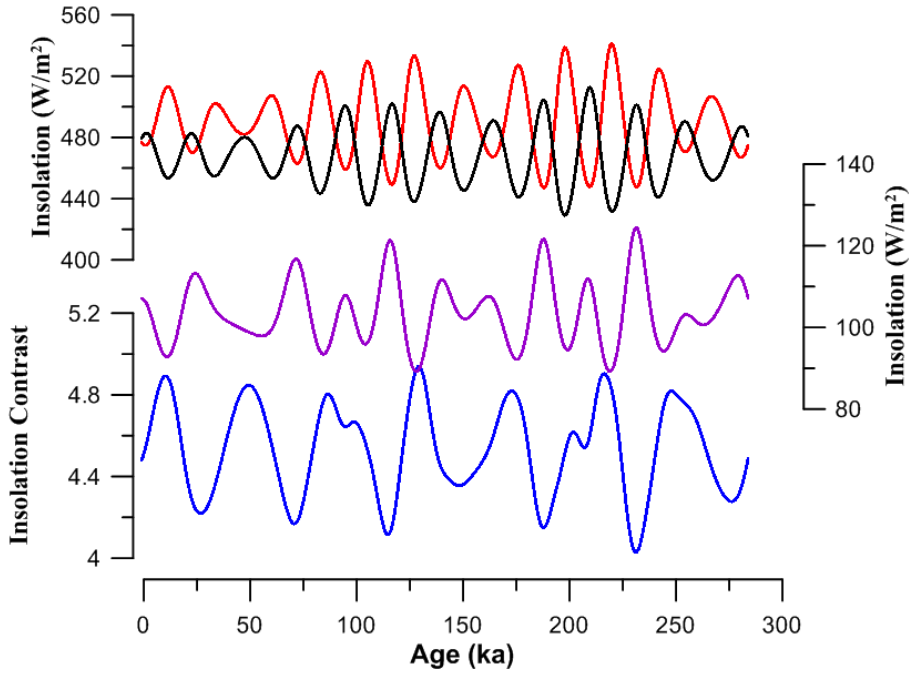

Fig. 8. Orbital insolation: (1) 30° N June insolation (red); (2) 20° S December insolation (black); (3) 50° N December insolation (purple); contrast between (2) and (3) (blue).

CPD
7, 943–964, 2011